

Molecular Dynamics Simulations of the Ionic Liquid [EMIM⁺][TFMSI⁻] Confined Inside Rutile (110) Slit Nanopores

Ramesh Singh,^{1,2,*} Nav Nidhi Rajput,^{1,*} Xiaoxia He,¹ Jermain Franklin,^{1,†} Joshua Monk^{1,3} and Francisco R. Hung¹

¹ Cain Department of Chemical Engineering, Louisiana State University, Baton Rouge, LA 70803

² Department of Chemical and Biomolecular Engineering, University of Notre Dame, Notre Dame, IN 46556

³ Thermal Protection Materials Branch, NASA Ames Research Center, Moffett Field, CA 94035

Abstract: The structure and dynamics of the ionic liquid (IL) [EMIM⁺][TFMSI⁻] inside a rutile (110) slit nanopore of width $H = 5.2$ nm at $T = 333$ K are studied using classical molecular dynamics (MD) simulations. These results are compared against those obtained in our previous study (Rajput *et al.*, *J. Phys. Chem. C* **2012**, *116*, 14504-14513) for the same IL inside a slit graphitic nanopore of the same width. Our results suggest that the strength of the interactions between the pore walls and the IL can significantly affect the structure and dynamics of the confined IL. Layering effects were more pronounced for the IL inside a rutile pore as compared to inside a graphitic pore. The dynamics of the IL inside a slit rutile pore are significantly slower than those observed inside a slit graphitic pore.

Keywords: ionic liquid; rutile; molecular dynamics simulations

1. Introduction

Ionic liquids (ILs) are molten salts typically composed of bulky organic cations with smaller organic or inorganic anions, and usually are in liquid phase near room temperatures. ILs have attracted interest for applications as alternative electrolytes in electrochemical double layer capacitors (EDLCs)^{1, 2} and dye-sensitized solar cells (DSSCs).³⁻⁷ In EDLCs and DSSCs, the IL is in contact with a nanoporous electrode, and therefore a fundamental understanding of the properties of ILs inside nm-sized pores is crucial to rationally design EDLCs and DSSCs, and significantly advance those technologies. Molecular simulations are well positioned to make important contributions towards achieving a fundamental understanding of the interfacial properties of ILs near nanoporous electrodes. Previous simulation studies from our group⁸⁻¹² focused on understanding the structure and dynamics of ILs inside carbons with pores of different geometries. The main objective of this work is to study in detail the structural and dynamical properties of the IL 1-ethyl-3-methylimidazolium bis-(trifluoromethanesulfonyl) imide, [EMIM⁺][TFMSI⁻] confined inside a slit-like nanopore formed by two parallel (110) rutile TiO₂ walls. TiO₂ is one of the semiconductor materials that have been used extensively in DSSCs.^{3, 6, 7} Here we focused on [EMIM⁺][TFMSI⁻] inside a rutile slit pore with a pore width $H = 5.2$ nm, mainly to compare directly with our previous results¹¹ for the same IL inside carbon slit pores of different pore sizes, including $H = 5.2$ nm. This direct comparison would allow us to discuss the effects of the material of the pore walls, which affects the wall-IL interactions, on the structure and dynamics of the confined IL. The dynamics of ILs inside the nanopores determine the macroscopic electrical resistance in IL-based DSSCs. The structure of the IL inside the nanopores is relevant to processes such as charge screening and possible recombination processes involving the electrons, the dye and the IL electrolyte, which ultimately affect the efficiency of DSSCs.

* Equal contribution

† LA-SiGMA REU student, 2013

2. Computational Details

[EMIM⁺][TFMSI⁻] is initially placed inside the slit rutile pore, and various pore loadings ($0.6\rho_{\text{bulk}}$, $0.8\rho_{\text{bulk}}$ and ρ_{bulk} , where $\rho_{\text{bulk}} \sim 1.5 \text{ g/cm}^3$) were considered by changing the number of IL pairs inside the volume of the pore (Fig. 1). Periodic boundary conditions were applied in all directions. All our IL/rutile systems were placed in the center of an orthorhombic box; the total length of this box in the z direction was $L_z = 12 \text{ nm}$. Classical molecular dynamic (MD) simulations in the NVT ensemble were performed using the GROMACS MD package¹³ at $T = 333 \text{ K}$. The two pore walls are formed by repeating the rutile unit cell along the [100], [010], and [001] and then cutting the box along the (110) plane to form a slab of dimensions $5.6 \text{ nm} \times 5.1 \text{ nm}$. The O and Ti atoms in the rutile surface were modeled as LJ spheres with $\sigma_o = 0.303$, $\sigma_{Ti} = 0.392$, nm, $\epsilon_o = 0.12 \text{ kcal/mol}$, and $\epsilon_{Ti} = 0.041 \text{ kcal/mole}$ ^{14, 15}. The partial charges of O and Ti are $-1.098e$ and $2.196e$.¹⁶ The rest of our simulation details are exactly the same as used in our previous studies.^{11, 12}

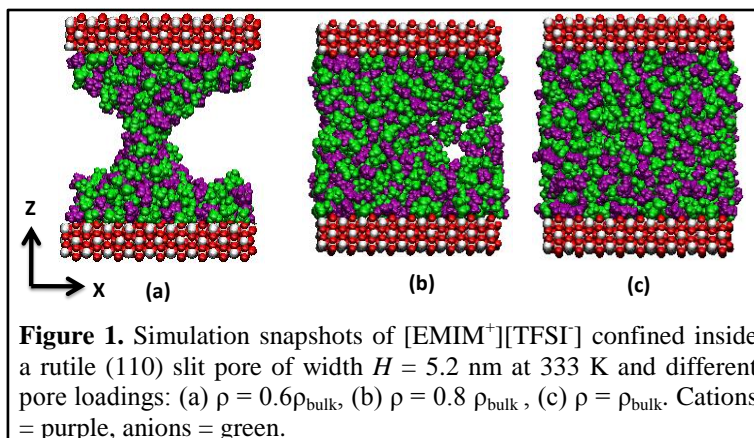


Figure 1. Simulation snapshots of [EMIM⁺][TFMSI⁻] confined inside a rutile (110) slit pore of width $H = 5.2 \text{ nm}$ at 333 K and different pore loadings: (a) $\rho = 0.6\rho_{\text{bulk}}$, (b) $\rho = 0.8\rho_{\text{bulk}}$, (c) $\rho = \rho_{\text{bulk}}$. Cations = purple, anions = green.

3. Results and Discussion

In Fig. 2 we present the number density profiles for the confined IL at various densities; snapshots of these systems are depicted in Figure 2. For $\rho = 0.6\rho_{\text{bulk}}$, the IL is mostly adsorbed near the pore walls, with the center regions of the pore partially depleted of IL (Figs. 1, 2). For this particular pore loading ($\rho = 0.6\rho_{\text{bulk}}$), the equilibrium configuration has inhomogeneities in the center of the pore, consisting of a liquid-like ‘bridge’ region and a vacuum-like region with almost no IL present. Increases in the amount of IL inside a rutile slit pore lead to increases in the density of IL in the center of the pore, but cause negligible changes in the density of ions near the pore walls (Fig. 3). For the same IL within a slit graphitic nanopore of the same width ($H = 5.2 \text{ nm}$), increases in the density of IL within the pore lead to increases in the local density of ions in the center of the pore and near the pore walls (see Figure 3 in ref. ¹¹). The differences between Fig. 2 and Fig. 3 from ref. ¹¹ might be caused by differences in the wall-IL interactions. Electrostatic and dispersion interactions are present between [EMIM⁺] (C, N and H atoms), [TFMSI⁻] (N, S, F, and O atoms) and the Ti and O atoms in the rutile walls; in contrast, only weaker van der Waals interactions are present between the ions and the C atoms in the graphitic walls. In Fig. 3 we show the mean square displacement (MSD) of the ions in the directions parallel to the rutile walls (x and y directions). Results are reported for the ions near the rutile walls (first layers) and in the center of the pore at

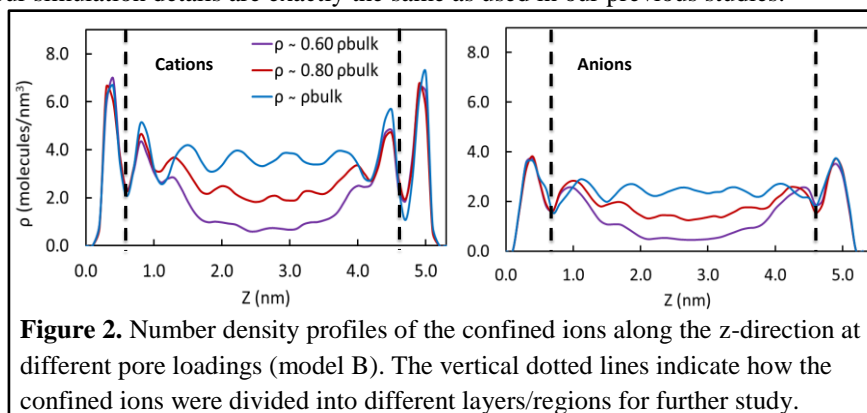


Figure 2. Number density profiles of the confined ions along the z -direction at different pore loadings (model B). The vertical dotted lines indicate how the confined ions were divided into different layers/regions for further study.

different pore loadings. We also ran a simulation at a density $\rho = 1.1\rho_{\text{bulk}}$ (labeled ‘model A’ in Fig. 3). These results suggest that the dynamics of the ions in the center of the pore do not depend monotonically on the amount of IL inside the pore. In all cases, the ions in the center of the pore have faster dynamics than the ions near the pore walls. Among the systems studied, the slowest dynamics were observed for both types of ions at $\rho = 1.1\rho_{\text{bulk}}$, mainly due to the high density of the confined ions. At $\rho \leq \rho_{\text{bulk}}$, the dynamics of the cations in all regions of the pore, and of the anions in the center of the pore, decrease monotonically with a reduction in pore loading; the fastest dynamics are observed for $\rho = \rho_{\text{bulk}}$, followed by $\rho = 0.8\rho_{\text{bulk}}$ and $\rho = 0.6\rho_{\text{bulk}}$ (the anions near the rutile walls follow a different trend, and we further discuss it below).

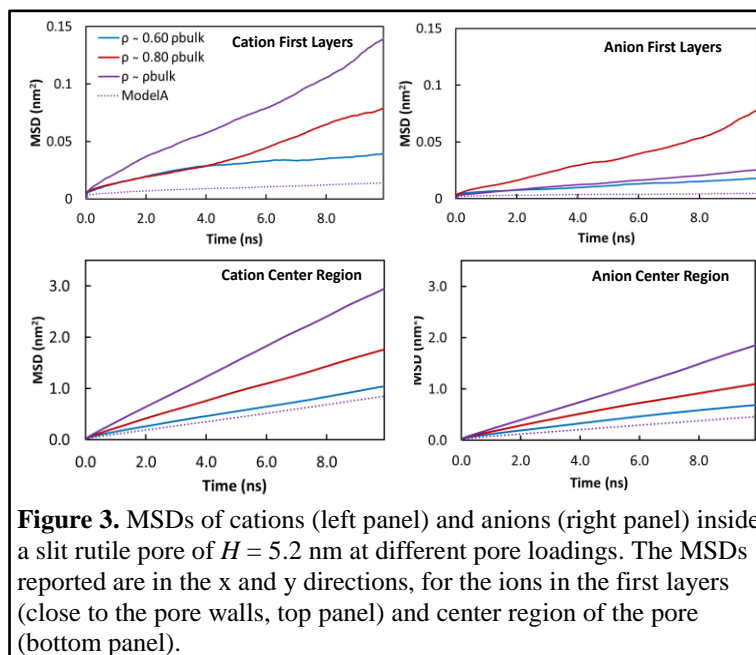


Figure 3. MSDs of cations (left panel) and anions (right panel) inside a slit rutile pore of $H = 5.2$ nm at different pore loadings. The MSDs reported are in the x and y directions, for the ions in the first layers (close to the pore walls, top panel) and center region of the pore (bottom panel).

The slower dynamics observed when we reduce the amounts of IL inside the pore might be due to the formation of inhomogeneous regions with low and high density of IL inside the pore (Fig. 1a). These trends agree with those observed for ILs inside carbon pores, in which reducing the amount of IL inside the pore beyond a certain percentage of ρ_{bulk} could lead to a slowdown in the dynamics of the confined ions. In Figure 3, the anions near the rutile walls follow a slightly different trend than anions in the center of the pore, and cations everywhere: the anions closest to the rutile walls in the system with $\rho = 0.8\rho_{\text{bulk}}$ exhibits the fastest dynamics, followed by $\rho = \rho_{\text{bulk}}$ and $\rho = 0.6\rho_{\text{bulk}}$. This behavior might be due to differences in the strength of interactions between the anions (F, C, S, O and N atoms) and the rutile walls (Ti, O atoms), as compared to the interactions between the walls and the cations (C, N and H atoms). The dynamics of [EMIM⁺][TFMSI] inside a slit rutile pore are significantly slower than those observed for the same IL inside a slit graphitic pore of the same size, $H = 5.2$ nm.¹¹ The dynamics of ions closest to the rutile walls are about an order of magnitude slower than those of ions closest to graphitic walls. The ions in the center of a rutile pore exhibit a slightly enhanced mobility, but their dynamics are about 2-4 times slower than those of ions in the center of a graphitic pore. These results suggest that the interactions of the pore walls with the IL ions can significantly affect the dynamics of the confined IL. The amount of IL inside the nanopores also induce heterogeneous dynamics, especially when highly inhomogeneous phases are observed such as those obtained for $\rho = 0.6\rho_{\text{bulk}}$ inside slit rutile pores (Fig. 1a) and inside slit graphitic pores (Fig. 4 in ref. ¹¹).

4. Concluding Remarks

The structure and dynamics of [EMIM⁺][TFMSI] inside a rutile (110) slit nanopore of width $H = 5.2$ nm at $T = 333$ K were studied using classical MD simulations. Our results were compared against those obtained in our previous study¹¹ of the same IL inside a slit graphitic nanopore of the same width and at the same temperature. Layering behavior was observed for [EMIM⁺][TFMSI] inside the slit rutile nanopore; formation of

layers was also observed for the same IL inside a slit graphitic pore,¹¹ but in the latter case layering effects were weaker in the center of the pore and two small density peaks were observed near the pore walls. Highly inhomogeneous phases consisting of a liquid-like ‘bridge’ and a vacuum-like region were observed for the confined IL at $\rho = 0.6\rho_{\text{bulk}}$ in the center of the slit rutile and carbon pores. The dynamics of [EMIM⁺][TFMSI⁻] inside a slit rutile pore are significantly slower than those observed for the same IL inside a slit graphitic pore of the same size, $H = 5.2$ nm.¹¹ The dynamics of ions closest to the rutile walls are about an order of magnitude slower than those of ions closest to graphitic walls. The ions in the center of a rutile pore exhibit a slightly enhanced mobility, but their dynamics are about 2-4 times slower than those of ions in the center of a graphitic pore. The effects of variations in the amount of IL inside a rutile pore on the dynamics were very marked, with reductions of up to 4 times in the mean squared displacements (MSDs) of the ions in the different regions of the pore; in contrast, pore loading seem to lead to smaller variations in the dynamics of ILs inside a graphitic slit nanopore.¹¹ Densities above ρ_{bulk} seem to induce a slowdown in the dynamics; the presence of inhomogeneous liquid and vacuum regions in the center of the pore at $\rho = 0.6\rho_{\text{bulk}}$ might be the cause of the slow dynamics observed here. These differences in structure and dynamics of the confined IL might be explained by the strength of the IL-walls interactions: strong electrostatic and dispersion interactions are present between the IL and the rutile walls, whereas only weaker van der Waals interactions are present between the IL and the graphitic walls. Overall, our results suggest that the structure and dynamics of confined ILs are a result of a complex interplay between different factors: (1) chemistry of the pore walls; (2) density of IL inside the nanopores; (3) distance of the ions to the pore walls; (4) pore size, shape and surface roughness; (5) electrical charges in the pore walls.

5. Acknowledgements

This work was partially supported by the NSF (EPSCoR Cooperative Agreement EPS-1003897 and CAREER Award CBET-1253075), and by the Louisiana Board of Regents. High-performance computational resources were provided by HPC at LSU (<http://www.hpc.lsu.edu>) and LONI (<http://www.loni.org>).

6. References

- [1] M. Armand, F. Endres, D. R. MacFarlane, H. Ohno and B. Scrosati, *Nat. Mater.* **8** (8), 621-629 (2009).
- [2] C. Largeot, C. Portet, J. Chmiola, P. L. Taberna, Y. Gogotsi and P. Simon, *Journal of the American Chemical Society* **130** (9), 2730-2731 (2008).
- [3] A. Hagfeldt, G. Boschloo, L. Sun, L. Kloo and H. Pettersson, *Chemical Reviews* **110** (11), 6595-6663 (2010).
- [4] Y. Cao, J. Zhang, Y. Bai, R. Li, S. M. Zakeeruddin, M. Grätzel and P. Wang, *The Journal of Physical Chemistry C* **112** (35), 13775-13781 (2008).
- [5] D. Kuang, P. Wang, S. Ito, S. M. Zakeeruddin and M. Grätzel, *Journal of the American Chemical Society* **128** (24), 7732-7733 (2006).
- [6] B. Liu and E. S. Aydil, *Journal of the American Chemical Society* **131** (11), 3985-3990 (2009).
- [7] P. V. Kamat, *Accounts Chem. Res.* **45** (11), 1906-1915 (2012).
- [8] R. Singh, J. Monk and F. R. Hung, *J. Phys. Chem. C* **114**, 15478-15485 (2010).
- [9] R. Singh, J. Monk and F. R. Hung, *J. Phys. Chem. C* **115** (33), 16544-16554 (2011).
- [10] J. Monk, R. Singh and F. R. Hung, *J. Phys. Chem. C* **115** (7), 3034-3042 (2011).
- [11] N. N. Rajput, J. Monk, R. Singh and F. R. Hung, *The Journal of Physical Chemistry C* **116** (8), 5169-5181 (2012).
- [12] N. N. Rajput, J. Monk and F. R. Hung, *J. Phys. Chem. C* **116** (27), 14504-14513 (2012).
- [13] B. Hess, C. Kutzner, D. van der Spoel and E. Lindahl, *Journal of Chemical Theory and Computation* **4** (3), 435-447 (2008).
- [14] T. Utesch, G. Daminelli and M. A. Mroginiski, *Langmuir* **27** (21), 13144-13153 (2011).
- [15] O. Borodin, G. D. Smith, R. Bandyopadhyaya and O. Bytner, *Macromolecules* **36** (20), 7873-7883 (2003).
- [16] A. V. Bandura and J. D. Kubicki, *The Journal of Physical Chemistry B* **107** (40), 11072-11081 (2003).